American Mineralogist, Volume 90, pages 1655–1660, 2005

Zoltaiite, a new barium-vanadium nesosubsilicate mineral from British Columbia: Description and crystal structure

PAUL R. BARTHOLOMEW,[1,*] FRANCO MANCINI,[2,†] CHRISTOPHER CAHILL,[3] GEORGE E. HARLOW,[2] AND HEINZ-JUERGEN BERNHARDT[4]

[1]Geology and Geophysics, University of Connecticut, Storrs, Connecticut 06269, U.S.A.
[2]Earth and Planetary Sciences, American Museum of Natural History, Central Park West at 79th Street, New York, New York 10024-5192, U.S.A.
[3]Department of Chemistry, George Washington University, 725 21st Street N.W., Washington, D.C. 20052, U.S.A.
[4]Zentrale Elektronen-Mikrosonde, Ruhr-University Bochum, Universitätsstrasse 150, 44801 Bochum, Germany

ABSTRACT

Zoltaiite, ideal formula $BaV_2^{4+}V_{12}^{3+}Si_2O_{27}$, space group $P\bar{3}$, $a = 7.601(1)$, $c = 9.219(1)$ Å, $V = 461.34(1)$ Å^3, $Z = 1$, is a new mineral found on the eastern edge of the Shuswap metamorphic complex of British Columbia, Canada. It is a metamorphic mineral formed under greenschist-facies *P-T* conditions as part of an assemblage that includes quartz, celsian, apatite, sphalerite, pyrrhotite, galena, and pyrite. Zoltaiite has a Mohs hardness of 6–7, no cleavage, an anhedral to semi-prismatic habit, and a calculated density of 4.83 g/cm^3. It is opaque with reflectance and color similar to those of sphalerite. The strongest eight lines of the X-ray powder diffraction pattern [*d* in Å (*I*) (*hkl*)] are 3.103(78)(021), 2.934(89)(2$\bar{1}$2), 2.785(67)(013), 2.679(48)(022), 2.403(50)(211), 2.190(100)(212), 1.934(53)(213), and 1.438(63)(140). The empirical formula, derived from electron-microprobe analysis and the crystal structure, is $Ba_{1.05}(Ti_{1.31}V^{4+}_{0.69})_{\Sigma 2.00}(V^{3+}_{11.06}Fe^{3+}_{0.49}Cr_{0.34})_{\Sigma 11.89}Si_{2.06}O_{27}$ based on O = 27. The crystal structure was solved by direct methods and refined on the basis of F_0^2 using all unique reflections measured with Mo*K*α X-radiation on a CCD-equipped diffractometer. The final *R* factor was 3.2%, calculated using 659 unique observed reflections. The unit cell contains four layers of two types parallel to (001): X, an octahedral and tetrahedral sheet, and Y, an octahedral plus barium sheet; both layers are doubled through inversion centers resulting in the sequence XXYY... Two consecutive equivalent layers are interconnected through shared octahedral edges, whereas consecutive non-equivalent layers are linked through shared corners. The high calculated density is consistent with the dense packing of the structure.

INTRODUCTION

Zoltaiite was discovered in a single rock sample from the Wigwam Pb-Zn deposit in southeastern British Columbia, Canada. This rock sample was contributed to the first author by Dr. Trygve Höy of the B.C. Geological Survey in response to a request for samples for a survey study of sphalerite geobarometry. Although the rock was not found to be suitable for sphalerite geobarometry, in the process of surveying the assemblage using backscattered electron (BSE) imaging and energy dispersive X-ray spectrometry (EDS), a mineral with very unusual vanadium-rich chemistry was noticed. Subsequent quantitative electron microprobe analyses made it clear that this was a new mineral.

The new mineral is named after Tibor Zoltai (1925–2003) in recognition of his contributions to mineralogy both as a researcher and as an educator. The IMA Commission on New Minerals and Mineral Names has approved the new mineral and the name. Among his contributions, Zoltai solved the structure of coesite (Zoltai and Buerger 1959), refined the classification of silicates and other minerals with tetrahedral structures (Zoltai 1960; Zoltai and Buerger 1960), taught mineralogy to many undergraduate and graduate students, and co-authored a mineralogy textbook (Zoltai and Stout 1984).

* E-mail: pbartholomew@lycos.com
† Present address: U.O. Geologia, Italferr s.p.a., Via Marsala 53, 00185, Rome, Italy

GEOLOGIC SETTING

The Wigwam deposit is located in the Akolkolex River area southeast of Revelstoke, British Columbia. The Akolkolex River area, positioned along the transition between the Shuswap metamorphic complex and the Selkirk Mountain fold and thrust belt, is described by Thompson (1972, 1978) as a structurally complex package of metasediments of Cambrian to Ordovician age. The Wigwam deposit is contained within the Badshot Formation, which is associated with other occurrences of lead-zinc mineralization locally and throughout the Kootenay Arc (Thompson 1978; Höy 1982). Although the Badshot Formation is dominated by variably metamorphosed limestones, the sulfide mineralization is closely associated with a thin gray band of quartzite. The mineralization of the Wigwam Deposit, as well as minor mineralization in other parts of the Akolkolex River area, is associated with hinge zones of structural folds. The fact that the sulfide layers themselves are folded, and the dominance of pyrrhotite over pyrite, have been taken as indicating that the mineralization pre-dated regional metamorphism and folding (Muraro 1966; Thompson 1978). Pelitic rocks in the area contain an assemblage of quartz, albite, muscovite, and chlorite that is typical of the chlorite zone of greenschist-facies metamorphism; an analysis of regional metamorphism, including rocks of much higher grade to the west, traces out a *P-T* path that passes above the aluminosilicate triple point (Thompson 1972, 1978).

0003-004X/05/0010–1655$05.00/DOI: 10.2138/am.2005.1602

PARAGENESIS

Zoltaiite occurs with quartz, celsian, apatite, sphalerite, pyrrhotite, and galena as a disseminated mineral with an estimated modal abundance of 0.01%. Grains of zoltaiite occur most commonly within patches of sulfides that have minor admixed silicate grains. The general degree of grain-boundary regularity is typical of greenschist-facies metamorphism, and zoltaiite textures are consistent with being part of the equilibrium assemblage (Fig. 1). Zoltaiite grains average 60 μm in diameter but range from a few micrometers across to 200 μm. Many grains of zoltaiite are equant, but some are elongate and semi-prismatic (Fig. 2). Some of the largest grains of zoltaiite contain inclusions, mainly of pyrrhotite and occasionally of quartz.

Given that zoltaiite is part of the equilibrium metamorphic assemblage, the available descriptions of nearby metapelites and regional *P-T-t* path analysis (see above) make it possible to estimate broadly the *P-T* conditions of zoltaiite formation. The petrographic description of pelites near the Wigwam deposit by Thompson (1978) indicates a complete absence of biotite, thus implying that the metamorphic conditions were at temperatures below the "biotite-in" reaction of the greenschist facies (Bucher and Frey 2002). The bounds upon the metamorphic conditions implied by these conclusions (Fig. 3) lead us to estimate the *P-T* conditions of zoltaiite formation as 2 to 5 kbars and 300 to 425 °C.

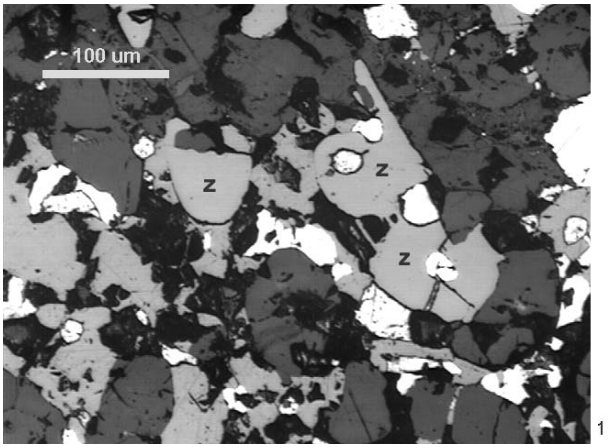

FIGURE 1. Reflected-light photomicrograph showing zoltaiite grains (Z) in the type sample.

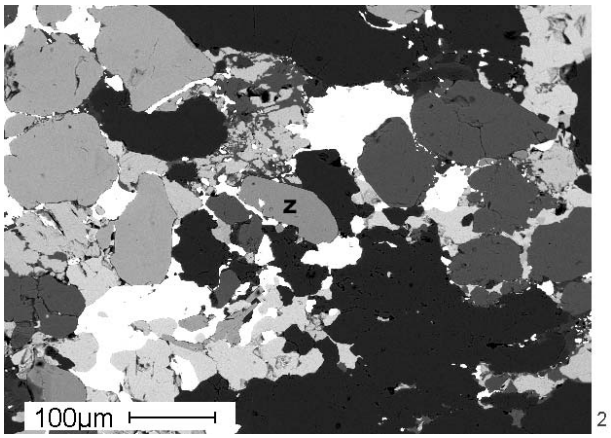

FIGURE 2. Backscattered-electron (BSE) micrograph of a zoltaiite grain (Z) in matrix, showing semi-prismatic form.

PHYSICAL PROPERTIES

Zoltaiite is black to steel gray and opaque, with a submetallic to dull luster. No cleavage was observed, and the fracture is irregular. Edge-relief formation and scratch resistance in polished sections, when compared to nearby known minerals, made it possible to estimate a Mohs hardness of 6-7. The measured chemical composition and unit-cell dimensions (see below) yield a calculated density of 4.83 g/cm^3. In reflected light, zoltaiite has a low reflectance (similar to that of sphalerite), a gray color with a weak brownish tint, no internal reflections, and weak anisotropy, bireflectance, and pleochroism.

Reflectance measurements were made with a custom-made reflectance microscope that uses 16 single-line interference filters (half-width 10 nm) with peak wavelengths between 400 and 700 nm in steps of 20 nm. The objective in air and immersion oil is 20× with an effective numerical aperture of 0.18 in air and in oil. The reflectance standard was SiC no. 878. Leitz immersion oil conforming to DIN 58884 was used. Color is given for illuminant C. The results are given in Table 1.

CHEMICAL COMPOSITION

Electron microprobe analyses of zoltaiite were obtained with the JEOL 8600 Superprobe at Yale University using a 15 kV, 30 nA beam. Qualitative analyses showed the presence of V, Ba, Ti, Si, Fe, Al, Mg, Cr, and O and ruled out detectable concentrations of all other elements heavier than C. Quantitative analyses took care to avoid spectral interferences between Ba*M*α-Ti*K*α, Ti*K*β-V*K*α, and V*K*β-Cr*K*α. Full ZAF matrix corrections were employed and oxygen was calculated by stoichiometry. Table 2 shows the average analysis of 14 separate grains of zoltaiite. The cation valences shown in Table 2 are those assumed for the purposes of

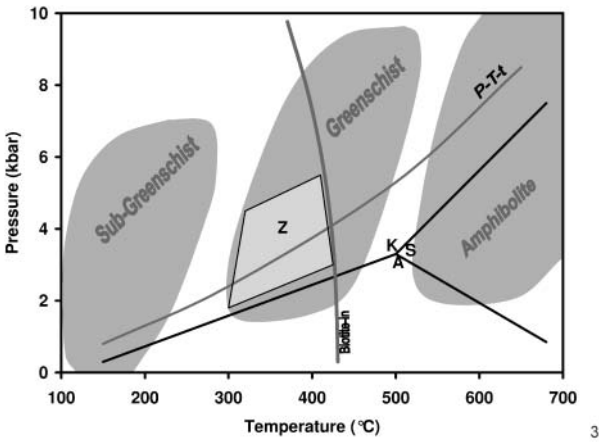

FIGURE 3. A *P-T* diagram, adapted from Bucher and Frey (2002) and Spear and Cheney (1989), showing the generally accepted range of conditions for the greenschist facies, the approximate position of the "biotite-in" reaction for pelites, the stability fields of kyanite (K), andalusite (A), and sillimanite (S), and a *P-T-t* path that is consistent with that of Thompson (1978). Also shown is the range of conditions most likely responsible for the formation of zoltaiite (Z).

calculating the oxygen content. Structural analysis (see below) both supports the 3+ valence assignment for Fe and requires that some of the vanadium be V^{4+}. This last requirement implies that the microprobe matrix-correction program, which accepts only one valence value per element, underestimated both the oxygen and the wt% total in Table 2.

STRUCTURE DETERMINATION

Single-crystal X-ray data

Single grains of zoltaiite were extracted by hand picking from polished thin sections. Electron microbeam EDS spectra were collected from individual grains both before and after the picking to make sure that only zoltaiite grains were selected. Grains verified to be zoltaiite were checked for sharpness of diffraction spots using a Buerger precession camera. A small crystal ($20 \times 20 \times 30$ μm) was selected and mounted on a Bruker four-circle goniometer equipped with a 1K SMART CCD detector with a crystal-detector distance of 5 cm. A hemisphere of data was collected using graphite-monochromatized Mo$K\alpha$ radiation and frame widths of 0.3° in ω, with 10 seconds/frame. A subset of reflections accounting for nearly half of the total number of reflections was identified that obeyed a single orientation matrix and gave a hexagonal unit cell with $a = 7.601(1)$ and $c = 9.219(1)$ Å. A total of 3059 reflections was collected in the Laue symmetry class –1 (no conditions) for $3° \le 2\theta \le 58.52°$. Intensities were integrated and corrected for Lorentz, polarization, and background effects using the Bruker program SAINT. The $|E^2 - 1|$ for all data, 0.949, fits the theoretical value for a centrosymmetric space group, $|E^2 - 1| = 0.968$ (i.e., for a non-centrosymmetric space group $|E^2 - 1| = 0.736$), and the complete reflection statistics supported the trigonal space group $P\bar{3}$ ($R_{int} = 6.3\%$). Data were re-indexed in the new setting. Merging equivalent reflections resulted in 792 unique reflections with 659 considered as observed ($|Fo| \ge 4\sigma_F$) for solution and refinement of the crystal structure. A summary of the data collection is presented in Table 3.

TABLE 1. Zoltaiite reflectance (%) and color values in air and immersion oil

Wavelength (nm)	air R_1	air R_2	oil R_1	oil R_2
400	16.00	16.43	4.43	4.91
420	15.82	16.38	4.40	4.94
440	15.79	16.53	4.43	5.07
460	15.83	16.70	4.49	5.21
470*	15.87	16.83	4.53	5.29
480	15.92	16.96	4.57	5.38
500	15.98	17.13	4.62	5.50
520	16.00	17.26	4.64	5.56
540	16.00	17.33	4.64	5.58
546*	15.99	17.33	4.64	5.58
560	15.96	17.31	4.63	5.59
580	15.94	17.37	4.62	5.62
589*	15.93	17.41	4.62	5.59
600	15.93	17.45	4.62	5.57
620	15.95	17.56	4.65	5.73
640	16.03	17.69	4.69	5.81
650*	16.08	17.75	4.72	5.85
660	16.14	17.81	4.76	5.90
680	16.26	17.91	4.85	5.97
700	16.40	18.03	4.92	6.02
		Color values		
x	0.311	0.314	0.313	0.318
y	0.318	0.321	0.321	0.326
Y(%)	15.97	17.33	4.63	5.60
Ld	566	574	570	574
Pe	0.67	2.56	2.09	4.88

* Interpolated value.

TABLE 2. Results from electron microprobe analyses

Constituent	Wt%	Standard deviation	Microprobe standard	Atoms per formula unit*
Mg^{2+}	0.06	0.006	chromite	0.03
Al^{3+}	0.03	0.006	chromite	0.02
Si^{4+}	4.21	0.11	fayalite	2.06
Ti^{4+}	4.55	0.21	rutile	1.31
V^{3+}	43.42	0.71	V_2O_5	11.74
Cr^{3+}	1.30	0.42	chromite	0.35
Fe^{3+}	1.99	0.07	hematite	0.49
Ba^{2+}	10.45	0.22	$BaAl_2O_4$	1.05
O^{2-}	31.03	0.23	By stoichiometry	
Total	97.04			

Note: All standards listed as mineral names are natural mineral standards.
* Atoms per formula are calculated on the basis of all cations (except Ba) = 16.

Structure refinement

The structure was solved by direct methods (SHELXS-86; Sheldrick 1986) using the scattering curves for neutral atoms and anomalous dispersion corrections (*International Tables for X-ray Crystallography*; Ibers and Hamilton 1974). Structure refinement (SHELXL97; Sheldrick 1997) using anisotropic temperature factors for all atoms yielded agreement factors R_u of 4.5% and 3.1% calculated respectively for all data and for the 659 "observed" reflections; the goodness of fit (S) was 1.001. Site-scattering indicated that V1 and V2 were predominantly occupied by vanadium, the Ba site by barium, and the Si site by silicon; thus, the occupancies of these sites were fixed at 1.0 in subsequent cycles of refinement. The V3 site was found to be occupied by both Ti and V (as indicated by the site-scattering and the mean bond length), and in subsequent refinement cycles their occupancies were considered as variables. The final atom parameters and displacement parameters are given in Tables 4 and 5, and selected interatomic distances, polyhedral volumes, and distortion parameters are in Table 6.

Powder X-ray data

Five of the hand-picked grains of zoltaiite were mounted together in a Gandolfi camera and exposed to Ni-filtered Cu radiation for 24 hours. The film was scanned, converted to a digital diffractogram with the program of Nguyen and Jeanloz (1993),

TABLE 3. Crystal data and refinement parameters

Crystal size (μm)	$20 \times 20 \times 30$
Crystal color	Black
Space group	$P\bar{3}$ (No.147)
a (Å)	7.601(1)
c (Å)	9.219(1)
V (Å^3)	461.34
*Density (g/cm^3)	4.83
Wavelength (Å)	0.71070
Diffractometer	Bruker $P4$ 1K Smart CCD
Scan mode $\Delta\omega = \Delta\phi$(°)	0.3
T(K)	293
$2\theta_{max}$(°)	58.52
$hkl_{(total)}$	3059
$hkl_{(unique)}$	792
$hkl_{(unique)}$ ($\|F_0\| > 4\sigma F_0$)	659
R	0.031
wR^2	0.066

* Density calculated assuming 100% occupancy.

TABLE 4. Atomic coordinates and isotropic temperature factors (Å^2) for zoltaiite

Site	x	y	z	U_{eq}*
Ba	0	0	1/2	0.0095(2)
V1	0.2070(1)	0.9557(1)	0.1377(1)	0.0065(2)
V2	0.0869(1)	0.4589(1)	0.6355(1)	0.00712)
V3	1/3	2/3	0.3578(1)	0.0083(4)
Si	1/3	2/3	0.9409(2)	0.0066(4)
O1	0.1777(6)	0.7455(4)	0.9908(3)	0.0073(6)
O2	0.2957(4)	0.4474(4)	0.5043(3)	0.0091(7)
O3	2/3	1/3	0.2402(5)	0.0076(11)
O4	0.0385(4)	0.2255(4)	0.7511(3)	0.0076(6)
O5	0.0952(4)	0.4839(4)	0.2593(3)	0.0080(6)
O6	0	0	0	0.0066(15)

* $U_{eq} = 8\pi^2\mu^2$.

TABLE 5. Anisotropic thermal parameters (Å²) for zoltaiite

Site	U_{11}	U_{22}	U_{33}	U_{23}	U_{13}	U_{12}
Ba	0.0100(2)	0.0100(2)	0.0085(3)	0	0	0.0050(1)
V1	0.0066(4)	0.0055(4)	0.0068(3)	0.0003(2)	0.0006(2)	0.0026(3)
V2	0.0079(4)	0.0063(4)	0.0071(3)	0.0002(2)	0.0007(2)	0.0034(3)
V3	0.0082(5)	0.0082(5)	0.0087(7)	0	0	0.0041(3)
Si	0.0078(7)	0.0078(7)	0.0042(9)	0	0	0.0039(3)
O1	0.0072(16)	0.0070(16)	0.0087(15)	–0.0010(11)	0.0007(11)	0.0044(14)
O2	0.0097(17)	0.0072(17)	0.0083(15)	0.0008(11)	0.0003(11)	0.0025(14)
O3	0.0086(17)	0.0086(17)	0.0057(24)	0	0	0.0043(8)
O4	0.0087(16)	0.0095(16)	0.0063(10)	–0.0009(11)	–0.0014(11)	0.0058(14)
O5	0.0085(16)	0.0083(16)	0.0074(15)	–0.0037(11)	–0.0006(11)	0.0042(14)
O6	0.0046(24)	0.0046(24)	0.0105(36)	0	0	0.0023(11)

TABLE 6. Selected interatomic distances (Å), polyhedral volumes (Å³), and distortion indices for zoltaiite

Ba-O4 (×6)	2.808(3)	V3-05 (×3)	1.874(3)
Ba-O2 (×6)	2.996(3)	V3-02 (×3)	2.051(3)
<Ba-O>	2.902	<V3-O>	1.962
		Quad. elon. (λ)	1.014
V1-04a	1.964(3)	Angle vari. (σ_θ)	42.720
V1-04b	1.978(3)	V(Å³)	9.904
V1-05c	1.961(3)		
V1-01d	2.020(3)	Si-O1 (×3)	1.637(3)
V1-01e	2.072(3)	Si-O3h	1.671(5)
V1-06f	2.175(1)	<Si-O>	1.645
<V1-O>	2.028	Quad. elon. (λ)	1.002
Quad. elon. (λ)	1.009	Angle vari. (σ_θ)	11.441
Angle vari. (σ_θ)	27.361	V(Å³)	2.277
V(Å³)	11.004		
V2-05a	1.909(3)		
V2-04	1.940(3)		
V2-02	2.032(3)		
V2-02c	2.065(3)		
V2-02g	2.059(3)		
V2-03h	2.087(2)		
<V2-O>	2.015		
Quad. elon. (λ)	1.008		
Angle vari. (σ_θ)	24.581		
V(Å³)	10.797		

Notes: $a = -x, -y + 1, -z$; $b = y, -x + y + 1, -z + 1$; $c = -x + y, -x + 1, z$; $d = x, y, z - 1$; $e = x - y + 1, x + 1, -z + 1$; $f = x, y - 1, z$; $g = x - y, x, -z + 1$; $h = -x + 1, y + 1, -z + 1$; $i = -y + 1, x - y + 1, z$.

TABLE 7. Indexed powder XRD data for zoltaiite

I_{obs}	d_{meas}	I_{calc}	d_{calc}	*hkl*
18	9.26	32	9.22	001
13	6.63	13	6.583	100
5	5.33	5	5.358	101, 011
34	3.796	19	3.801	110
		10	3.776	102, 012
17	3.517	18	3.514	111, 211
		2	3.292	200
78	3.103	74	3.1	021, 210
89	2.934	96	2.933	212, 112
67	2.785	83	2.785	013, 103
48	2.679	46	2.679	022, 202
12	2.488	11	2.488	210, 120
50	2.403	53	2.402	211, 121, 311, 131
		8	2.194	300
100	2.190	100	2.19	212, 312, 132
		4	2.175	104, 014
3	2.134	6	2.135	301, 031
16	1.980	21	1.981	032
8	1.971	9	1.971	114, 214
53	1.934	50	1.934	213, 133
16	1.902	5	1.9	220
		5	1.888	204
10	1.792	4	1.791	311
10	1.776	10	1.776	015, 105
9	1.758	8	1.757	422
45	1.693	40	1.691	214, 124
22	1.571	13	1.57	413, 133
31	1.492	10	1.49	251, 321
35	1.483	45	1.481	215,1r35
12	1.452	12	1.451	043, 403
63	1.438	47	1.437	140, 410
16	1.424	6	1.425	116, 216

TABLE 8. Site occupancies vs. calculated (calc) and observed (obs) octahedral mean bond lengths for zoltaiite

Site	Occupancy	<V-O>obs	<V-O>calc
V1	$0.93V^{3+}+0.07Cr^{3+}$	2.028	2.038
V2	$0.92V^{3+}+0.08Fe^{3+}$	2.015	2.032
V3	$0.67Ti^{4+}+0.33V^{4+}$	1.962	1.950

and then run through XFIT (Coelho and Cheary 1996) to fit the peaks. A sixth grain of zoltaiite was added to the mount and the process was repeated. Observed intensities and measured *d* values from the two films were averaged; the results are shown in Table 7, which includes a powder pattern calculated from the structure refinement data with XPOW (Downs et al. 1993). Excluded from Table 7 are two low-intensity peaks present in the Gandolfi films that were not present in the calculated powder pattern and probably result from inclusions commonly observed in zoltaiite: quartz (d = 3.35) and pyrrhotite (d = 2.056).

Coordination of the cations

In zoltaiite, there are three distinct octahedrally coordinated vanadium sites: V1 and V2, 6 cations each per unit cell, are at general positions; V3, with 2 per unit cell, resides on the threefold axis. Silicon resides on the triad in a tetrahedrally coordinated site, two atoms per unit cell, and a single Ba atom lies on an inversion center in ~12-fold coordination. Electroneutrality requires that 12 of the 14 V sites contain 3+ valence, and that the other 2 contain 4+ valence (Table 8). The bond lengths and bond valences both point to the two V3 sites as the locus of 4+ valence. Thus, the general zoltaiite structural formula is $BaV_2^{4+}V_{12}^{3+}Si_2O_{27}$. The chemistry and structure topology of zoltaiite would classify it as a nesosubsilicate according to Strunz (1996).

The Ba atom is coordinated as a trigonal antiprism by O4 at 2.80 Å within a girdle of six O2, at 2.99 Å on the equatorial plane. The bond-valence sum for all twelve ligands is high for Ba^{2+} (Table 9), suggesting non-bonding and potential displacement from some equatorial O2 bonds; however, neither residual electron densities nor anisotropy of the displacement parameters (Table 5) indicate positional disorder (i.e., site splitting).

The SiO_4 is a regular tetrahedron (<Si-O> = 1.645 Å) with one longish bond of 1.671 Å to the apical oxygen, and three short bonds of 1.637 Å. The refined scattering, ~14 e^-, and the mean bond length indicate that this site is occupied entirely by Si, consistent with the absence of other light scatterers in the chemical analysis of zoltaiite (Table 2).

For V1 and V2, site-scattering refinement yields ~23e^- for each, indicating occupancy mainly by V^{3+}. There is a minor difference in <V-O> distances, 2.028 and 2.015 Å for V1 and V2, respectively, whereas the sum of ionic radii for V^{3+} and O^{2-} is 2.040 Å (Shannon 1976), thereby suggesting additional occupancy by smaller cations. The potential candidates are Cr and Fe (Table 2), with Mg and Al ignored because of their very low concentrations. With respect to the valence state of Fe, although the mixed valence of V would suggest a reducing environment, Fe^{3+} is preferred on the basis of electroneutrality and ionic radius. Thus, cations were assigned to the V1 and V2 sites by fixing V^{3+} and Fe^{3+} from the microprobe analyses and adjusting the Cr^{3+} to yield full occupancy. Between

V1 and V2, the latter has the shortest mean bond length, suggesting that Fe^{3+} (0.69 Å) enters this site whereas Cr^{3+} (0.75 Å) is concentrated at V1. The good agreement between observed and calculated mean bond lengths supports these assignments (Table 8).

For the V3 site, the bond-valence sum and refined scattering of ~22e^- indicate occupancy by Ti^{4+} (0.74 Å) and V^{4+} (0.72 Å). The refined Ti^{4+} occupancy of ~0.66, or 1.34 apfu, is consistent with the microprobe data (1.31 Ti^{4+} apfu - Table 2), thereby supporting the proposal that one-third of V3 is occupied by V^{4+} and two-thirds by Ti. Likewise, the average <V-O> distance calculated using these occupancies, 1.950 Å, matches the observed value (Table 8). Further support for this cation assignment is given by consideration of polyhedral distortion; whereas V1 and V2 contain trivalent V and are nearly regular octahedra with a restricted range of V-O distances (Table 6), V3 is slightly more distorted due to 1/3 occupancy of this site by V^{4+}.

TABLE 9. Calculated bond valences (v.u.) for zoltaiite

	O1	O2	O3	O4	O5	O6	
Ba		0.149 $^{\times 6\rightarrow}$		0.243 $^{\times 6\rightarrow}$			2.352
V1	(0.473+ 0.411)		(0.550+ 0.530)	0.555	0.311 $^{\times 6\downarrow}$	2.830	
V2		(0.458+ 0.419+ 0.426)	0.396 $^{\times 3\downarrow}$	0.587	0.638		2.924
V 3		0.509 $^{\times 3\rightarrow}$			0.822 $^{\times 3\rightarrow}$		3.993
Si	1.011 $^{\times 3\rightarrow}$		0.920				3.953
	1.895	1.961	2.108	1.910	2.015	1.866	

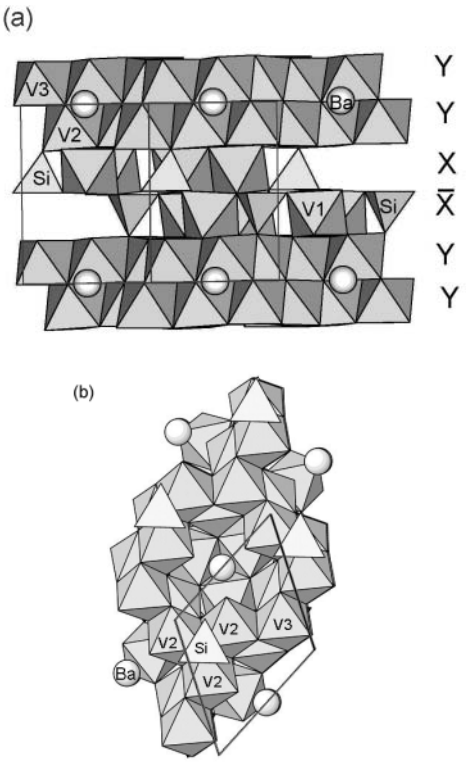

FIGURE 4. Polyhedral representations of the structure of zoltaiite. (**a**) Projected along [100], and (**b**) projected along [001]. For clarity, no polyhedra are drawn around the Ba atom (white circles). The letters X and Y in (**a**) designate the layer type (see text).

Structure topology

The structure is based on close-packed layers of oxygen atoms parallel to (001) and consists of a stack of four layers of two types (Figs. 4a and 4b): X, an octahedra plus tetrahedra sheet, and Y, an octahedra plus barium sheet. Each layer, X and Y, is doubled through the inversion center, respectively at O6 and Ba, resulting in the sequence XXYYXX... Two consecutive equivalent layers (i.e., X-X or Y-Y) are connected by shared octahedral edges, whereas two consecutive non-equivalent layers (i.e., X-Y) are connected by shared corners. In the X layer, the V1 octahedron shares edges to form $V1_3O_{13}$ clusters; linkage between clusters within the sheet occurs by sharing corners with the base of SiO_4 tetrahedra in voids in the sheet (Fig. 5a). "Bridging" SiO_4 tetrahedra in adjacent X layers point alternately up and down and share an apical O3 with three V2 cations of the Y layers above and below. In total, each V1 octahedron shares four edges (two basal and two lateral) with other V1 octahedra. In the Y layer, V2 octahedra share edges to form $V2_3O_{13}$ clusters with a common corner at O3. These clusters are linked to each other by sharing a lateral edge with a "bridging" V3 octahedron, and Ba occurs at the center of cavities in the layer formed by cluster of three empty octahedra (Fig. 5b). Each V2 octahedron shares three edges (two lateral and one basal) with other V2 octahedra and two edges (one lateral and one basal) with a "bridging" V3 octahedron; in turn each V3 octahedron shares six edges (three lateral and three basal) with V2 octahedra.

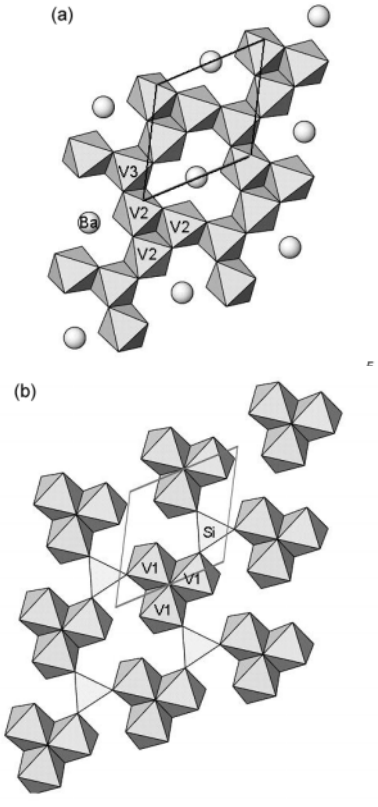

FIGURE 5. Polyhedral representations of the two non-equivalent layers in zoltaiite. (**a**) The X layer analogous to the octahedral layer forming synadelphite and phase-A; (**b**) the Y layer analogous to the layers found in hematolite and welinite (see text).

DISCUSSION

Relationship to other V minerals

In terms of vanadium valences alone, zoltaiite is nearly unique among vanadium minerals. Extracting all of the vanadium and vanadium-bearing minerals from an online mineral database such as Webmineral (Barthelmy 2004) and subtracting those that are not oxides and those containing less than 2 wt% V results in 154 species. Of these species, 93 contain only V^{5+}, 20 contain only V^{4+}, 26 contain only V^{3+}, and 14 contain both V^{5+} and V^{4+}. Only häggite, like zoltaiite, contains both V^{3+} and V^{4+}.

With its multiplicity of oxidation states, vanadium yields a large number of compounds, natural and synthetic, formed by different coordination polyhedral types that correlate with its oxidation state (Zavalij and Whittingham 1999; Schindler et al. 2000). In agreement with the prevalence of V^{3+} in the structure, zoltaiite belongs to the "O" class of vanadium structures (Zavalij and Whittingham 1999), built from sheets of octahedra defined by the close-packed layers of anions that share edges to form a three dimensional framework (Fig. 5). The Y layer can be described as a regular octahedral sheet in which 3/7 of all octahedra defined by the close-packed layers of anions, that is V1, are occupied by V^{3+}. Analogously, the X layer forms a regular octahedral sheet in which 4/7 of the octahedral cavities are filled; V^{3+} occupies V2 whereas V^{4+} enters V3. Comparison with other V^{4+}-bearing minerals would predict for V3 a greater distortion (e.g., a square dipyramid), which in zoltaiite is possibly compensated by Ti^{4+} that occupies about 66% of this site.

Related structures

The close-packing of the structure of zoltaiite is evident from the density of 4.83 g/cm^3. Aspects of the densely coordinated sheet structures in this mineral exist in the structures of hematolite $[(Mn^{2+},Mg,Al)_{15}(OH)_{23}(AsO_3)(AsO_4)_2]$, welinite $[Mn_6(W,Mg)_2Si_2(O,OH)_{14}]$, synadelphite $[Mn_9(OH)_9(H_2O)_2(AsO_3)(AsO_4)_2]$, and high-pressure phase-A $[2Mg_2SiO_4{\cdot}3Mg(OH)_2]$, all containing analogous layers (modular units) (Moore 1970; Moore and Araki 1978; Horiuchi et al. 1979). The X layer is analogous to the sheets-forming phase-A and synadelphite, except that the SiO_4 tetrahedron is replaced by $(AsO_4)^{3-}$ in synadelphite. Noteworthy is that the SiO_4 tetrahedron of zoltaiite, which shares only corners with octahedra, has the same local geometry as that found in phase-A. Accordingly, the Si-O(basal) and Si-O(apical) bond distances are very similar in the two minerals. The Y layer is analogous to that found in hematolite and welinite (Moore and Araki 1978), but AsO_4 and SiO_4 tetrahedra in these two structures occupy part of the Ba polyhedron which, to be precise, is a $Ba(O4)_3$ polygon. The $Ba(O4)_3$ unit, which shares corners with octahedra, has the same local environment as that of the SiO_4 tetrahedron in welinite. Moreover, the V3 octahedron of zoltaiite is analogous to M1 in welinite (Moore 1970) in that it accommodates cations of higher charge (i.e., Mn^{4+} in welinite) and plays a structurally similar "bridging" role.

Thus, a family of structures, both real and potential, with moderate complexity and chemical diversity can be constructed from combinations of layers (modular units) of similar topology. However, comparison of zoltaiite with related compounds shows differences in local geometries. First, the SiO_4 tetrahedron in $BaV_{14}Si_2O_{27}$ is corner-shared whereas the $(AsO_4)^{3-}$ tetrahedron in synadelphite is edge-shared, possibly resulting from the greater cation-cation repulsion of Si^{4+}-$[V^{3+}]^{V2}$ and Si^{4+}-$[V^{4+}]^{V3}$ vs. As^{5+}-Mg^{2+} in the respective structures. Second, consecutive layers in zoltaiite are linked by edge and corner sharing, respectively, whereas between layers in welinite and hematolite some octahedra share faces, which again probably results from greater V^{3+}-V^{3+} (and V^{3+}-V^{4+}) repulsion compared with Mg^{2+}-Mg^{2+}.

ACKNOWLEDGMENTS

Many thanks to T. Höy and the B.C. Geological Survey for contributing the type rock sample. We thank C. Prewitt for allowing access to the X-ray facilities at the Geophysical Laboratory, Carnegie Institution of Washington. F.M. gratefully acknowledges support through a Coleman post-doctoral fellowship at the AMNH. F.M is also grateful to H. Papunen (Turku University, Finland) for sharing interest in mineralogy and much more. P.B. thanks A. Philpotts for the loan of photomicroscopy equipment.

REFERENCES CITED

Barthelmy, D. (2004) Mineralogy Database. (http://webmineral.com/).
Bucher, K. and Frey, M. (2002) Petrogenesis of Metamorphic Rocks, Seventh Edition. Springer Verlag, Berlin.
Coelho, A.A. and Cheary, R.W. (1996) X-ray Line Profile Fitting Program, XFIT. Deposited in CCP14 Powder Diffraction Library, Engineering and Physical Sciences Research Council, Daresbury Laboratory, Warrington, England. (http://www.ccp14.ac.uk/tutorial/xfit-95/xfit.htm).
Downs, R.T., Bartelmehs, K.L., Gibbs, G.V., and Boisen, M.B., Jr. (1993) Interactive software for calculating and displaying X-ray or neutron powder diffractometer patterns of crystalline materials. American Mineralogist, 78, 1104–1107.
Horiuchi, H., Morimoto, N., Yamamoto, K., and Akimoto, S. (1979) Crystal structure of $2Mg_2SiO_4{\cdot}3Mg(OH)_2$, a new high-pressure structure type. American Mineralogist, 64, 593–598.
Höy, T. (1982) Stratigraphic and structural setting of stratabound lead-zinc deposits in southeastern B.C. CIM Bulletin, 75, 114–134.
Ibers, J.A. and Hamilton, W.D., Eds. (1974) International Tables for Crystallography, IV. Kynoch Press, Birmingham, U.K.
Moore, P.B. (1970) Crystal chemistry of the basic manganese arsenates. IV. Mixed arsenic valences in the crystal structure of synadelphite. American Mineralogist, 55, 2023–2037.
Moore, P.B. and Araki, T. (1978) Hematolite: a complex dense-packed sheet structure. American Mineralogist, 63, 150–159.
Muraro, T.W. (1966) Metamorphism of zinc-lead deposits in southeastern British Columbia. CIM Special Volume, 8, 239–247.
Nguyen, J.H. and Jeanloz, R. (1993) A computer program to analyze X-ray diffraction films. Review of Scientific Instruments, 64, 3456–3461.
Schindler, M., Hawthorne, F.C., and Baur, W.H. (2000) Crystal chemical aspects of vanadium: polyhedral geometries, characteristic bond valences, and polymerization of (VO_n) polyhedra. Chemical Materials, 12, 1248–1259.
Shannon, R.D. (1976) Revised effective ionic radii and systematic studies of interatomic distances in halides and chalcogenides. Acta Crystallographica, A32, 751–767.
Sheldrick, G. (1986) SHELXS-86. Program for crystal structure solution. University of Göttingen, Germany.
——— (1997) SHELXL-97: A computer program for structure refinement. University of Göttingen, Germany.
Spear, F.S. and Cheney J.T. (1989) A petrogenetic grid for pelitic schists in the system SiO_2-Al_2O_3-FeO-MgO-K_2O-H_2O. Contributions to Mineralogy and Petrology, 101, 149–164.
Strunz, H. (1996) Chemical-structural mineral classification. Principles and summary of system. Neues Jahrbuch fur Mineralogie, Monatshefte, 10, 435-445.
Thompson, R.I. (1972) Geology of the Akolkolex River area near Revelstoke, British Columbia, 125 p. Ph.D. thesis, Queen's University, Kingston, Ontario.
——— (1978) Geology of the Akolkolex River Area. British Columbia Ministry of Energy, Mines and Petroleum Resources, Bulletin 60, 84 p.
Zavalij, P.J. and Whittingham, M.S. (1999) Structural chemistry of vanadium oxides with open frameworks. Acta Crystallographica, B55, 627–663.
Zoltai, T. (1960) Classification of silicates and other minerals with tetrahedral structures. American Mineralogist, 45, 960–973.
Zoltai, T. and Buerger, M.J. (1959) The crystal structure of coesite, the dense, high-pressure form of silica. Zeitschrift für Kristallographie, 111, 129–141.
——— (1960) The relative energies of rings of tetrahedra. Zeitschrift für Kristallographie, 114, 1–8.
Zoltai, T. and Stout, J.H. (1984) Mineralogy: Concepts and Principles. Burgess, Minneapolis.

MANUSCRIPT RECEIVED JANUARY 13, 2004
MANUSCRIPT ACCEPTED FEBRUARY 17, 2005
MANUSCRIPT HANDLED BY LEE GROAT